Volume 17, No 2 | International Journal of Radiation Research, April 2019

A Monte Carlo simulation study on the effectiveness of electron filters designed for telecobalt radiation therapy treatment

R. Shukla[1], N.P. Patel[2*], H.P. Yadav[1], V. Kaushal[2]

[1]Department of Radiotherapy, GGS Medical College, Faridkot, India
[2]Department of Radiotherapy, Pt. B D Sharma Post Graduate Institute of Medical Sciences, Rohtak, India

► ***Original article***

Corresponding authors:
Dr. Narayan Prasad Patel,
Fax: *+91 1262 282 035*
E-mail:
nppatel03@hotmail.com

Revised: August 2017
Accepted: January 2018
Int. J. Radiat. Res., April 2019; 17(2): 217-227
DOI: 10.18869/acadpub.ijrr.17.2.217

ABSTRACT

Background*:** The aim of present study was to analyze the effectiveness of electron filters in the Telecobalt radiotherapy treatment by simulation technique. ***Materials and Methods*:** The BEAMnrc Monte Carlo code was used to simulate the electron filters of thickness of 0.5 gm/cm^2 below the trimmer bar for 35 × 35 cm^2 field size in Theratron Equinox-80 telecobalt unit. The electron filters were made of an aluminum, copper, nickel, tin, PMMA, and lead with single or composite materials. The radiation beams at treatment distance were analyzed by generating profiles for photon and electron along the X-axis of radiation field. ***Results: The electron energy fluence for unfiltered beam was 0.32% of the photon energy. The photon energy fluence intensity reduction due to filter was 3.7%. The filters with low atomic number have shown poor electron contamination removal efficiency. The tin, copper and nickel were found effective filters, removing nearly 38% of contaminant electron energy. The lead filter is equally effective as tin, however the high energy electrons emitted from filter due to "photo peaks" adds significant dose at 3.0 to 4.0 mm depth. ***Conclusion:*** The tin filter dominates over to other filters on the subject of surface dose reduction and depth of dose maximum (d_{max}). It reduces the surface dose by 9.6% and 13.9 % of unfiltered beam for 15 × 15 and 20 × 20 cm^2 field sizes respectively.

Keywords: *Telecobalt, electron contamination, electron filters, surface dose, Monte Carlo simulation.*

INTRODUCTION

The telecobalt machine is in use for cancer management for a long period due to its cost effectiveness. Its use in cancer treatment strikes the right balance between the technology and the art of medicine, with special relevance to radiotherapy [1]. A local and indigenous made new telecobalt unit is being promoted for more cost effective treatment of cancer patients [2]. The new advanced treatment modalities are also being facilitated in telecobalt machine for effective treatment of cancer [3-5].

The cobalt-60 source emits photons of energies of 1.17 and 1.33 MeV and beta particle of maximum energy of 0.31 MeV. The radiation beam incident on patient from the telecobalt machine is often contaminated with secondary electrons and low energy photons. The sources of the secondary contaminated electrons are source material, primary collimator, jaws, trimmer bars and air. The source capsule itself is major source of electron and photon contamination [6]. Because of these scattered photons and contaminant electrons, there is a change in the shape of depth-dose curve in the buildup region and shift in dose maximum point. Hence, the loss in the skin sparing effect is the main disadvantage of telecobalt and as well as megavoltage radiotherapy. Several authors have investigated the electron contamination in cobalt-60 and high energy X-ray beam and also

investigated various methods for removal of the electron contamination [6-14]. The electron contamination has also been removed to reduce the dose in buildup region that enhance the photon beam quality specification in high energy X-ray beam [15-18].

Rogers et al. have carried out the simulation based study on the effect of photon and electron contamination on surface dose in cobalt-60 beam [6]. They studied the removal of electron contamination by filters and magnets, and the results were compared with published experimental data. Leung et al. have performed an extensive study on effect of field sizes on electron contamination and filtration by various filters in cobalt-60 beam [7]. They recommended the use of medium atomic number filters of thickness of 0.4 g/cm^2 for cobalt-60 beam. Hueng et al. and Bova et al. have done the comparative study between acrylic and lead acrylic filter in ^{60}Co and high energy X-ray beam [8, 9]. Attix *et al.* included the helium gas filled bag and the metallic filters in the ^{60}Co beam [10]. Nilsson used the Fermi-Eyges theory of multiple scattering for relative lateral electron surface dose distributions from filters and air [11].

The most of the previous studies on electron contamination in telecobalt unit were ion chamber based experimental work [7-10]. The present study was planned to carry out the detail simulation study on various filter materials. The EGSnrc code coupled with BEAMnrc Monte Carlo simulation code is one of the most accurate technique for the simulation of electron dosimetry in radiotherapy units [19-20]. The BEAMdp programme of the BEAMnrc system is a prominent tool for the analysis of different parameters of photon and electron spectra [21]. The Theratron Equimox-80 from Best Theratronics, Ottawa, Canada is one of latest telecobalt unit used for the treatment of cancer. Various filters made of low to high atomic number, including tin of medium atomic number have been taken in this study. The aim of the study was to investigate the effectiveness of filter materials on removal of electron contamination in cobalt-60 beam and choose an appropriate filter material.

MATERIALS AND METHODS

Simulation codes

The simulation codes used in the present study were BEAMnrc and DOSXYZnrc. These codes were installed in the computer system of Intel i5-4570@3.2GHz processor with 4GB RAM system. The BEAMnrc code is able to handle the various geometries such as collimator, jaws, mirror, MLC etc. and coupled with EGSnrc user-code for the simulation of electron-photon transport, to simulate the radiation beams including high energy electron and photon beams from radiotherapy units [20-23]. The radiation beam was analyzed by BEAMdp data processor program that derive the spectral, planner fluence distribution of spectrum of photons and electrons [21]. The dose calculation in water phantom was performed using DOSXYZnrc general purpose Monte Carlo EGSnrc user-code [24].

Simulation of treatment unit and phantom

The study on the effectiveness of electron filters was performed by simulating filters in Theratron Equinox-80 telecobalt machine. The details regarding simulation of source, source housing, fixed and movable collimator is presented elsewhere [25]. These include the component module (CM) FLATFILT to model source capsule and surrounding lead shield (20 cm), the CM PYRAMIDS to model primary definer and the CM JAWS to model secondary collimator and trimmer bars. The jaws and trimmer bars were set to define the field size of 35 × 35 cm^2 at 80 cm treatment distance. The electron filter of dimension of 40 × 40 cm^2 was simulated by CM of SLABS below the last X-axis trimmer bars at 53.4 cm. The geometry of the simulation of complete system is shown in figure 1.

The DOSXYZnrc code was used to design virtual homogenous water phantom of volume of 40 × 40 × 20 cm^3 with source to surface distance of 80 cm. The height of the phantom was 20 cm and divided in the 400 thin layers of uniform thickness of 0.05 cm. The volume of water phantom was divided into large number of small

voxels. The dimensions (x × y × z) of the voxels were taken 1.0 × 1.0 × 0.05 cm^3 distributed uniformly over the phantom. The total number of dose scoring regions including exterior was 672401. The medium of the phantom was water with density of 1.0 g/cc.

Design of electron filters

The list of electron filters used in the present study, their density, composition and thickness is shown in table 1. The materials include PMMA, aluminum, nickel, copper, tin, and lead. The composite filters of two different materials were also used in this study. These include copper-aluminium, aluminium-copper and lead-PMMA combinations. Total ten filters were taken in this study. The density thickness of the filter was taken 0.5 gm/cm^2 for all the filters. An acrylic (PMMA) plate of 0.9 cm thickness supplied as standard accessory with the Theratron Equinox-80 machine and PMMA of 0.42 cm thickness were included in this study. The composite filter lead-PMMA with 60% density thickness of lead and 40% density thickness of PMMA was taken as filter. The composite filter of the combination of aluminum (0.148 cm) and copper (0.011 cm) with two different orientations were also included in the study.

Simulation process

The process of MC simulation was divided in three different steps. In the first step, the phase space file (PSF) was generated at plane 1 and plane 2 for unfiltered beam as shown in figure 1. In the simulation process, 10^{10} histories from the isotropic cylindrical source were run with default setting of the transport parameters of EGSnrc code. The particles reaching to plane 1 and plane 2 after passing through source capsule, primary definer, jaws and trimmer bar were scored in the PSF. The file contains the information about charge, energy, and moving direction of the particle. The typical simulation time to generate PSF of 3.7 GB at plane 2 was 160 hrs.

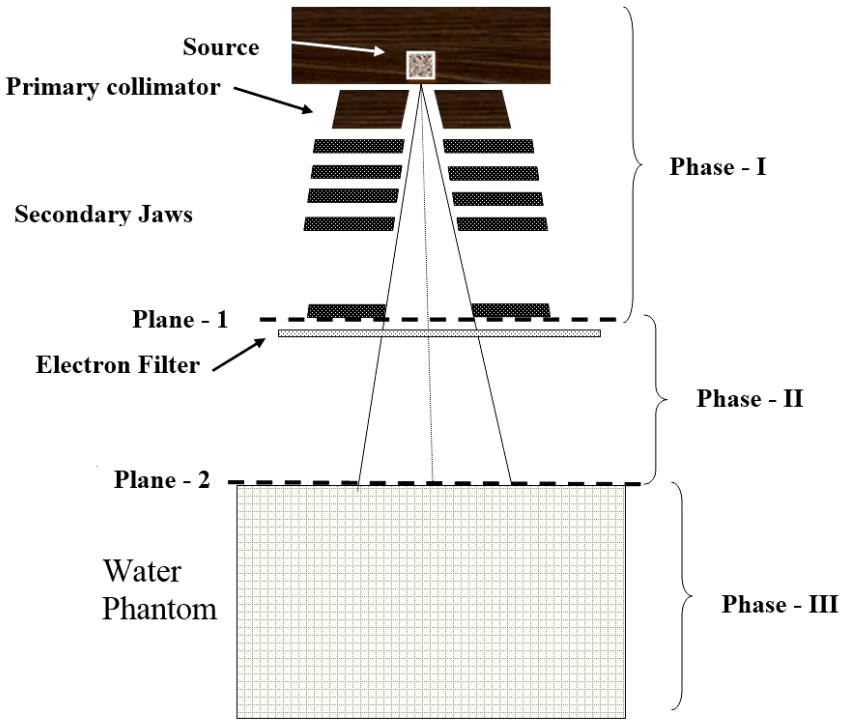

Figure 1. The geometry and configuration of the Theratron Equinox-80 machine in present simulation.

Table 1. The density, thickness and composition of various filters.

Sr. No.	Filter material (Element / Alloy)	Atomic number and composition	Density (g/cc)	Thickness (cm)
Element				
1	Aluminium	Al(13) = 0.99	2.71	0.185
2	Tin (Sn)	Sn (50) = 1.00	7.31	0.0684
3	Lead (Pb)	Pb (82) = 1.00	11.34	0.044
Alloy				
4	PMMA_0.42 ($C_5H_8O_2$)	H(1) =0.0805, C(6) =0.599 O(8) = 0.3196 Z_{eff} = 3.5	1.19	0.42
5	PMMA_0.9 ($C_5H_8O_2$)	-----	1.19	0.9
6	Nickel	Ni (28) =0.66 Cu(29)=0.287 Fe(26) =0.025 Mn(25) = 0.02 Si(14) = 0.005 C(6) = 0.003	8.902	0.056
7	Copper	Cu(29) = 0.85 Zn(30) = 0.15	8.75	0.0558
Composite filters				
8	Copper -Aluminum (Cu-Al)	0.1 gm/cm^2 Cu + 0.4 gm/cm^2 Al	8.75, 2.71	0.011 +0.148
9	Aluminum- Copper (Al-Cu)	0.4 gm/cm^2 Al + 0.1 gm/cm^2 Cu	2.71, 8.75	0.148+0.011
10	Lead-PMMA	0.3 gm/cm^2 Pb + 0.2 gm/cm^2 MMA	11.34 +1.19	0.026+0.168

In the second step, the component module SLAB was used to simulate the filters and air medium. The medium air was simulated between z = 49.67 and z = 53.4 cm from the source, and then filter was simulated as per the thickness and material composition as given in table 1. The medium between the filter and plane 2 at 80 cm from the source was taken air which was simulated by SLAB. In this process, the PSF generated at plane 1 was used as the source input file, and all particles photon, electron and positron were transported through filters and air to generate the second PSF at plane 2. The simulation process was run for 1.5×10^8 histories over 2.5 hrs for 3.7GB PSF size. The simulation parameters were similar to the parameters taken in step 1. The PSFs generated at the plane 2 at 80 cm for filters and without filter were analyzed to determine the effectiveness of the various electron filters.

In the third and final step, the absorbed dose (Gy/incident particle) was calculated to find out the depth-dose curve in the water phantom. The PSF at plane 2 was chosen as source file which was placed at the surface of water phantom. All the particles (photons, electrons and positrons) were set to incident on the water phantom. The numbers of particles present in the PSF were taken into account to decide the number of histories for the simulation in each calculation. This maintains the uniformity of the recycling of the particles present in PSF. The transport parameters ECUT and PCUT for the simulation were 0.521 and 0.01 MeV respectively. Total about 2.5×10^9 histories were simulated for each filter to achieve higher accuracy in dose values. The accuracy level achieved were 1.0% for the depth from 0.3 mm to 1.5 cm and 1.5 % at the surface level. The dose values along the central Z -axis were listed in pegslst file. The similar dose calculation in water phantom for all the filters and unfiltered beam were performed by simulation of the only photon particles in PSF.

RESULTS

The PSFs for 35 × 35 cm^2 filed size were generated at 80 cm for comparison between various filters and without filter data. The filter

was placed below the trimmer bar at 53.4 cm from the source. The statistical uncertainty of the results directly depends up on the number of particle histories used in the simulation. Hence, in order to improve the accuracy and minimize the error, 10^{10} particle histories from source were simulated to generate PSF at plane 1 and plane 2. The BEAMdp program was used to generate the various profiles for radiation beam along X-axis at 80 cm. These profiles include photon fluence vs. position, photon energy fluence vs. position, electron fluence vs. position, and electron energy fleuence vs. position plots. The profiles of mean energy of the electron and photon spectra for different filters were also analyzed. The other profile includes the energy distribution for the photon and electron spectra.

The profiles of photon fluence (fluence/ incident particle) vs. position and photon energy fluence (MeV/cm^2/incident particle) vs. position for the different filters and without filter are shown in figure 2(a) and 2(b) respectively. In the profile of photon fluence, the filters have shown variation in the particle filtration. The lead and PMMA_0.9 have shown the maximum decrease in the particle fluence. In the photon energy fluence vs. position, the energy fluence at the central axis for unfiltered beam was 1.12e-05 MeV per incident particle. The high Z and low Z filters are very close for the attenuation of photon energy fluence. The PMMA_0.9 filter of 0.9 cm has shown higher attenuation due to higher thickness. The decrease in photon energy fluence is about 3.7% for various filters with higher atomic number except PMMA_0.9 filter.

The profiles of electron fluence (fluence/ cm^2/incident particle) vs. position and electron energy fluence (MeV/cm^2/incident particle) vs. position for the different filters and without filter are shown in figure 3(a) and 3(b) respectively. The electron energy fluence is maximum at central axis and decreases gradually off-axis. The electron energy fluence along the central axis for unfiltered beam is 3.56e-08 MeV/cm^2 /incident particle. The filters with low atomic number have shown the low electron removal efficiency. The lead, aluminum and copper_aluminium have shown the moderate electron removal efficiency. The lead, PMMA and aluminium filters were found to be less efficient for removal of electron contamination for particle as well as energy fluence. The electron energy fluence for tin, copper and nickel were found 2.2e-08, 2.4e-08 and 2.6e-08 respectively. These filters are effective for the filtration of electron contamination, removing about 38% of electron energy compare to radiation beam without filter. The mean energy profile for photon and electron for open beam were 1.03 and 0.58 MeV respectively. The lead filter is observed to be beam hardener with mean energy for photon and electron of 1.05 and 0.62 MeV respectively. The filters with low atomic number and higher thickness such as PMMA, copper and aluminium were having low mean energy for photon as well as electron. The photon and electron mean energy was 1.00 MeV and 0.5 MeV respectively. These filters behave as scatterer than the attenuator for both photon and electron. The mean energy for photon and electron for tin filter were 1.02 and 0.58 MeV respectively, which is relatively higher compare to other low atomic filters.

The profiles of photon and electron energy fluence distribution for various filters and without filter are shown in figure 4(a) and 4(b) respectively. It is a particle energy fluence scored in user defined field vs energy with 200 energy bins of equal bin width within a specified field size in X-axis. The fluence peaks for photon were at energy level of 1.17 and 1.33 MeV respectively. The low energy photons were found in the energy range of 0.2 to 1.17 MeV. The filters with low atomic number and higher thickness show increase in low energy photon components in the energy range of 0.4 to 0.6 MeV. The lead and tin filters show energy fluence distribution as similar to the beam without filter. The electron energy fluence was 0.8 MeV for various filters and without filter. The filtration of the electron energy increases with increase in energy. The lead and tin have higher filtration of electron energy from unfiltered beam. The lead filter has shown two energy fluence peaks at 1.12 and 1.26 MeV. These peaks were not observed in unfiltered

beam.

The absorbed dose (Gy/incident particle) was calculated at different depths between zero to 2.0 cm in phantom. The calculation was made for photon and all particles (Photon, electron and positron) for filtered and unfiltered beam. The depth doses were normalized with the dose at depth of dose maximum (d_{max}). The relative depth-doses along the central axis for photon only and for all particles for all filters and unfiltered beam are shown in figure 5(a) and 5 (b) respectively. In case of photon beam only, the dose curves for the filtered and unfiltered beams are similar. The surface dose starts at 26% and attain maximum at 4.0 mm depth and falls at the same rate for all beams. The depth-dose due to photon, electron and positron for filters and unfiltered beam shows large deviation. The surface dose for unfiltered beam is 76% and reaches maximum at 0.125 cm depth. The surface dose for tin, copper, lead and nickel filters were 56.9%, 59.7%, 61.8% and 64.0% respectively. The d_{max} for tin, nickel and copper filter were 0.575, 0.475, and 0.275 cm respectively. The depth-dose results for other mostly used clinical field sizes 10 × 10, 15 × 15, and 20 × 20 cm^2 for unfiltered beam and filtered with tin is shown in figure 6 along with the field size of 35 × 35 cm^2. The surface dose for three field sizes were 37.3%, 48.8%, and 58.8% respectively. The d_{max} was 4.0 mm approximately for all. The surface dose reductions by the tin filter were 3.3%, 9.6% and 13.9% for above three field sizes respectively.

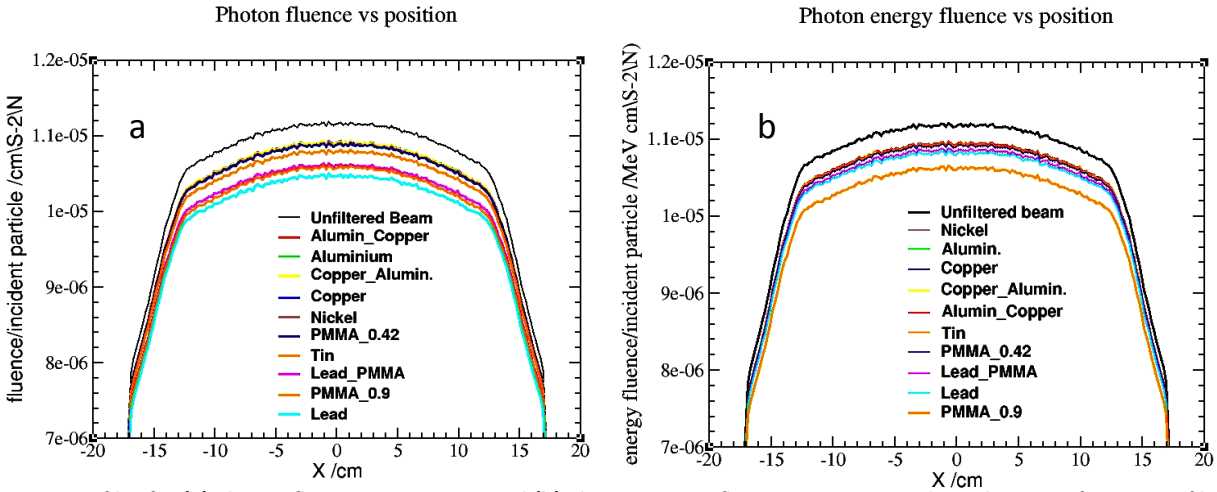

Figure 2. Profiles for **(a)** Photon fluence vs. position and **(b)** Photon energy fluence vs. position along the x-axis for various filters and without filter at treatment distance of 80 cm from the source.

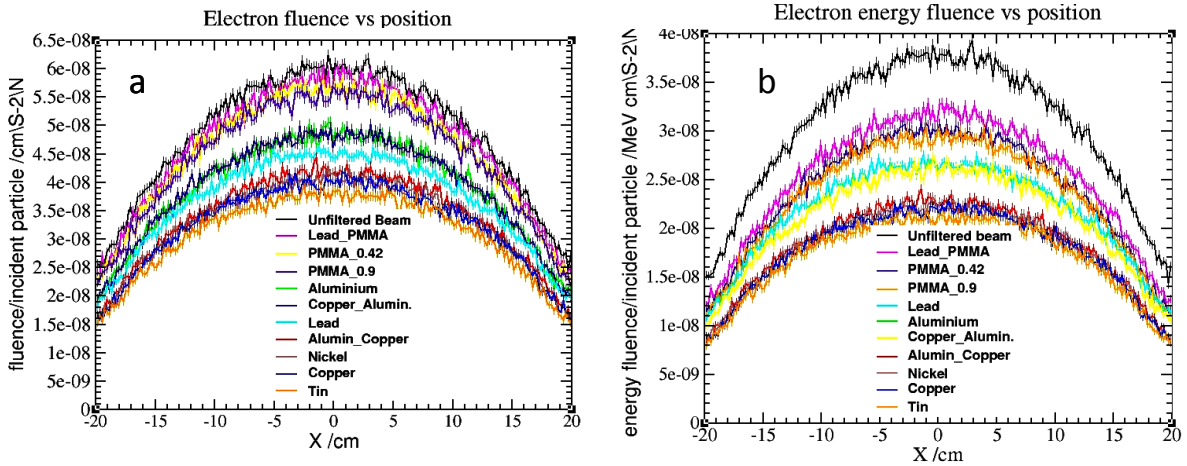

Figure 3. Profiles for **(a)** Electron fluence vs. position and **(b)** Electron energy fluence vs. position along the x-axis for various filters and without filter at treatment distance.

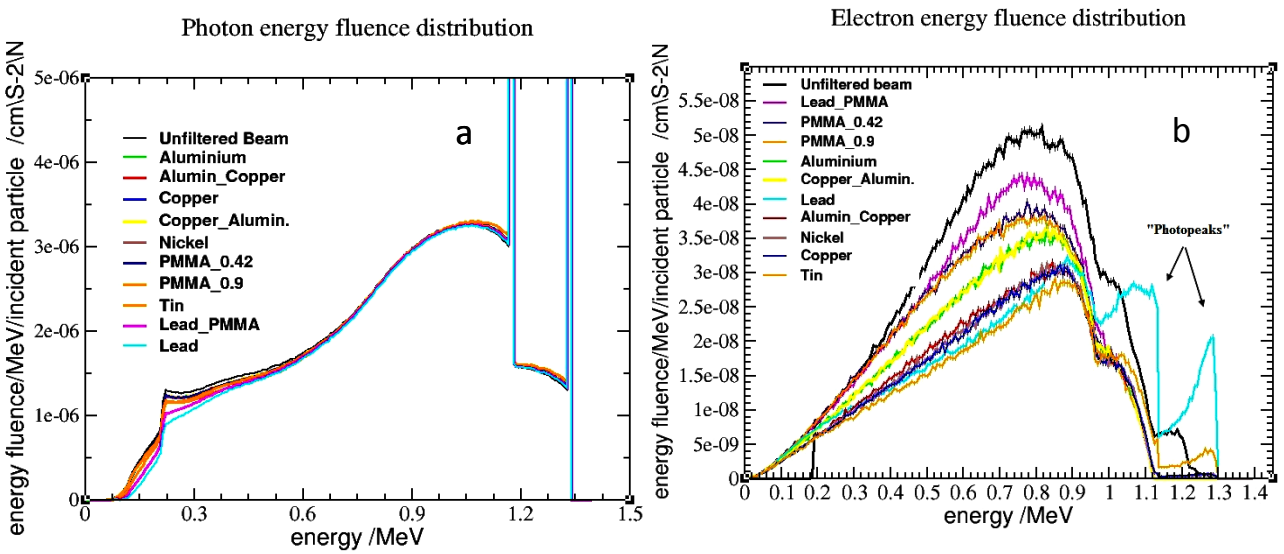

Figure 4. Profiles of energy fluence distribution for **(a)** Photon and **(b)** Electron along the x-axis for various filters and without filter at treatment distance.

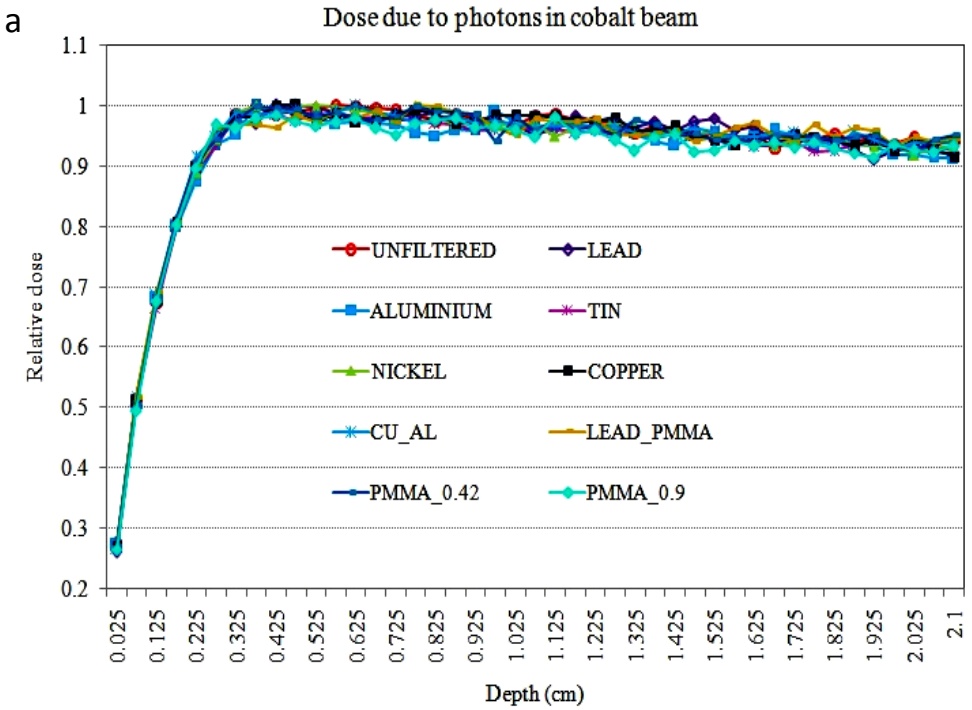

Figure 5. figure legend is described in next page.

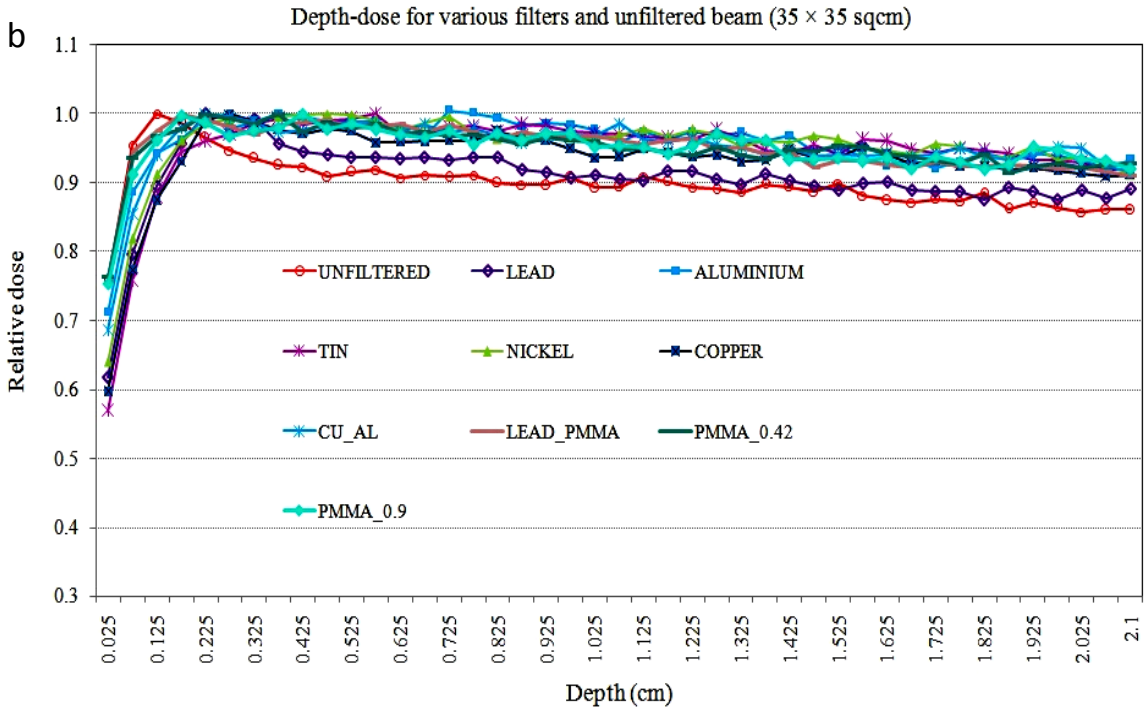

Figure 5. Depth-dose distributions for various filters and unfiltered beams for 35 × 35 cm^2 field size **(a)** for only due to photons in the beam and **(b)** due to all particles photon, electron and positron in the beam.

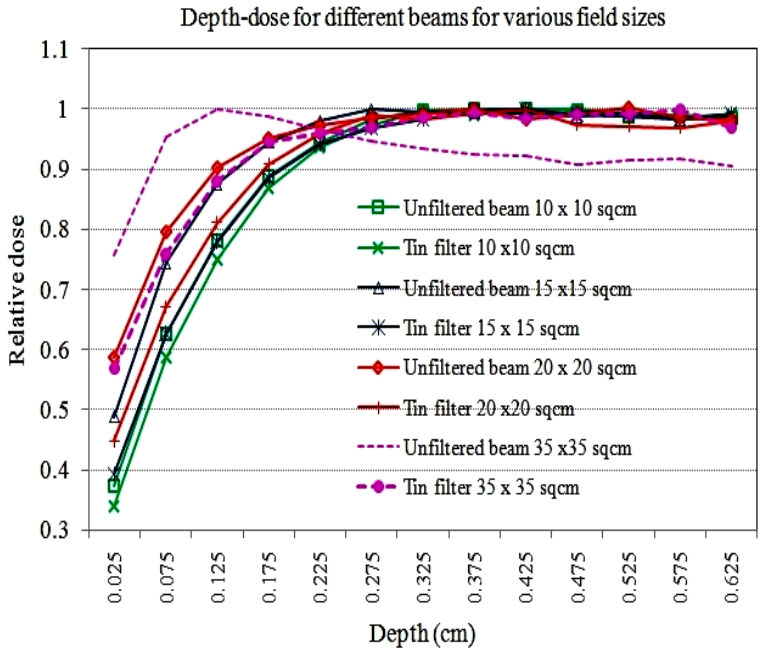

Figure 6. Depth-dose distribution in build-up region for all particles for tin filter and unfiltered beam for various field sizes.

DISCUSSION

The methods which have been applied for the study of filtration of electron contamination were thin metallic filters, use of magnet and helium filled polythene bag. The helium filled polythene bag is effective for removal of electron contamination; however it generates and scatter the electron at larger filled sizes [10]. The use of magnet is excellent for improvement in the beam characteristics of Co-60 and high energy X-rays, however its routine use is not feasible [11, 12]. The electron contamination varies with field size and the distance from the source. The most of the previous studies on the electron filters for Co-60 beam were ion chamber based for various field sizes and various distances using different materials [7-10]. The simulation technique was used in the present study for various filter materials for a large field size with maximum electron contamination. The accuracy of modeling of Equinox machine was validated by comparison of dosimetric calculation of output factors and the depth-dose data with measured values [25]. All the filters were simulated under the similar parameters and with single PSF below the trimmer bar.

Rogers *et al.* have found copper as better filter compare to PMMA in the study of photon and electron contamination on depth-dose curve in AECL ^{60}Co therapy unit using EGS simulation code [6]. The photon contamination is primarily from the source capsule, contributes significantly to the dose, but has less effect on the shape of depth-dose curve. The electron contamination comes from a wide variety of places; the capsule itself is the major source at close distances and air generated electrons dominate at larger distances. In the present simulation study, we have used several materials of filters from low to high atomic number for selection of appropriate material. The photon and electron spectra were deeply analyzed in BEAMdp programme for the validation of results. The surface depth-dose in water phantom clearly demonstrates the electron contamination removal efficiency of the filters. The d_{max} at 0.125 cm for unfiltered beam is in well agreement with result shown by Leung *et al.* [7]. The tin filter has significantly reduced the surface dose by 20% from the dose of unfiltered beam. The tin has not only decreased the surface dose but also increased the d_{max} from 0.125 cm to 0.575 cm. The shift in the d_{max} for smaller field for tin filter is not significant.

The copper and nickel have shown moderate filtration of electron contamination. The lead filter is marginally better compare to the PMMA and lead_PMMA filter. Attix et al. found that the copper and lead glass (L35C) shows strongest beam filtering action compare to Lucite as the PMMA adds more electron contamination than it removes [10]. The performance of above three filters is not satisfactory as reported by the authors [8, 9]. Huang et al. observed that lead acrylic is an effective filter compare to acrylic [8]. Bova *et al.* investigated that there is no clinical advantage in using either acrylic or lead acrylic over to the open tray system, however the use of lead acrylic as compared to acrylic demonstrated a decrease in surface dose and the dose at 1.0 mm depth for all of the photon energies [9].

The depth-dose in phantom is well correlated with the profiles for electron and photon spectra. The profile of electron energy fluence distribution in figure 4(b) shows that the tin and the lead filter shows the similar energy fluence till electron energy of 0.98 MeV, after that the lead filter shows two different electron energy fluence peaks at 1.12 and 1.26 MeV respectively. These two peaks are responsible for the increase in electron energy fluence for lead filter compare to the tin as shown in figure 3(b). The attenuation and scattering coefficient shows that the lead filter has clear edge over tin on the photoelectric effect. The two peaks in the profile of electron energy fluence distribution are "photo peaks" emitted due to interaction of gamma rays of cobalt-60 beam with the high Z lead filter. The range of these 1.12 and 1.26 MeV electrons in water is 3.0 to 4.0 mm. It shows that the lead filter adds the significant dose at 3.0 to 4.0 mm depth in phantom. Leung et al. also found that the lead filter gives higher dose at 3.0 to 4.0 mm due to "photo peaks" [7].

The result of the simulation study was validated by the measurement of depth-dose in

solid phantom using Markus parallel plate chamber for unfiltered beam using copper and perspex filter for 35 × 35 cm^2 field size in Theratron Equinox-80 machine. In the measurement setup, the source to detector distance was fixed at 80.5 cm and source to surface distance varies by placing the Perspex slabs of 0.1 cm thickness over detector. This measurement setup is not same as simulation of fixed source to surface distance, however it ensures the positional accuracy of the detector. The measured relative depth-dose for three beams is shown in figure 7. It is observed that the pattern of depth-dose curve for three different beams is similar as to the simulation result. There is deviation in the d_{max} and surface dose from simulation. This may be due to different measurement setup, thick slab layer and the uncertainty in water equivalency in phantom material. The d_{max} for unfiltered and copper filtered beams are 0.2 and 0.4 cm compare to 0.125 and 0.25 cm respectively of simulation results. The surface dose measured with parallel plate chamber having protective build up cap of 0.1 cm for three beams were in well agreement with the calculated dose absorbed in first layer of 0.05 cm thickness.

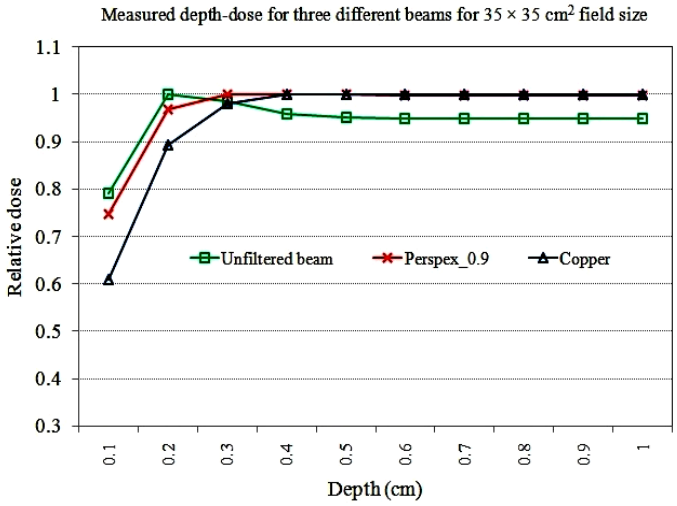

Figure 7. Measured relative depth-dose in solid phantom using parallel plate chamber for three different.

CONCLUSION

The present study concludes that the use of electron filters in telecobalt treatment is not clinically significant upto 10 ×10 cm^2 field sizes; however it should be used for higher field sizes. The medium atomic number filters have shown moderate efficiency for electron removal. The tin filter has shown maximum efficiency. The lead filter should not be used in telecobalt treatment.

***Conflicts of interest*:** *Declared none.*

REFERENCES

1. Ravichandran R (2009) Has the time come for doing away with Cobalt-60 teletherapy for cancer treatments. *J Med Phys, **34 (2)**: 63-65*.
2. Kumar R, Sharma SD, Phurailatpam R, Deshpande DD, Kannan S (2005) Performance characteristics of indigenously developed Bhabhatron-I telecobalt unit. *J Med Phys, **30**: 41-7*.
3. Schreiner LJ, Joshi CP, Darko J, Kerr A, Salomons G, Dhanesar S (2009) The role of Cobalt-60 in modern radiation therapy: Dose delivery and image guidance. *J Med Phys, **34(3)**: 133-36*.
4. Sahani G, Sharma SD, Dash Sharma PK, Sharma DN, Hussain SA (2013) Monte Carlo simulation based study of a proposed multilief collimator for a telecobalt machine.

Med Phys, ***40(2)****: 0217051-11*.
5. Joshi CP, Dhanesar S, Darko J, Kerr A, Vidyasagar PB and Shreiner LJ (2008) Practical and clinical considerations in Cobalt-60 tomotherapy. Souvenir and Book of Absracts, ICMP: *Mumbai; 13-4*.
6. Rogers DWO, Ewart GM, Bielajew AF (1988) Calculation of electron contamination in a cobalt-60 therapy beam. Proceeding of the symposium on dosimetry in radiotherapy. *IAEA,* ***1****: 303-12*.
7. Leung Philip MK, Johns HE (1977) Use of electron filters to improve buildup characteristics of large fields from cobalt-60 beams. *Med Phys,* ***4****: 441-44*.
8. Huang D, Williams S, Chaney E, Long F (1983) Evaluation of lead acrylic as a filter for contamination electrons in megavoltage photon beams. *Med Phys,* ***10****: 93-95*.
9. Bova FJ and Hill LW (1983) Surface doses for acrylic versus lead acrylic blocking trays for Co-60, 8-MV, and 17-MV photons. *Medical Physics,* ***10****: 254-56*.
10. Attix FH, Lopez F, Owolabi S, Paliwal BR (1983) Electron contamination in Co-60 gamma-ray beams. *Med Phys,* ***10****: 301-06*.
11. Nilsson B (1985) Electron contamination from different materials in high energy photon beams. *Physics in Medicine and Biology,* ***30(2)****: 139-52*.
12. Biggs PJ and Ling CC (1979) Electrons as the cause of the observed d_{max} shift with the field size in high energy photon beams. *Med Phys,* ***6****: 291-95*.
13. Ling CC and Biggs PJ (1979) Improving the buildup and depth-dose characteristics of high energy photon beams by using electron filters. *Med Phys,* ***6****: 296-301*.
14. Rao BM, Prasad SG, Parthasaradhi K, Lee Y, Ruparel R, Garces R (1988) Investigations on the near surface dose for three 10 MV X-ray beam accelerators with emphasis on the reduction of electron contamination. *Med Phys,* ***15****: 246-49*.
15. Parthasaradhi K, Prasad SG, Rao BM, Lee Y, Ruparel R, Garces R (1989) Investigation on the reduction of electron contamination with a 6 MV X-ray beam. *Med Phys,* ***16****: 123 -25*.
16. Ciesielski B, Reinstein LE, Wielopolski L, Meek A (1989) Dose enhancement in the buildup region by lead, aluminum, and lucite absorbers for 15 MV photon beam. *Med Phys,* ***16****: 609-13*.
17. Li XA and Rogers DWO (1994) Reducing electron contamination for photon beam-quality specification. *Med Phys,* ***21(6)****: 791-97*.
18. Roger DWO (1999) Correcting for electron contamination at dose maximum in photon beams. *Med Phys,* ***26 (4)****: 533 -37*.
19. Kawrakow I (2000) Accurate condensed history Monte Carlo simulation of electron transport. EGSnrc, the new EGS4 version. *Med Phys,* ***27****: 485 – 98*.
20. Rogers DWO, Faddegon BA, Ding GX, Ma CM, Wei JS, Mackie TR (1995) BEAM: a Monte Carlo code to simulate radiotherapy treatment units. *Med Phys,* ***22****: 503–25*.
21. Ma CM and Rogers DWO (2006) BEAMDP as a General Purpose utility. *NRCC Report PIRS-509(E) revA*.
22. Rogers DWO, Walters B, Kawrakow I (2005) BEAMnrc user's manual. *NRCC Report PIRS-0509(A). NRCC, Ottawa*.
23. Kawrakow I and Rogers DWO (2003) EGSnrc Code System. *NRCC report PIRS-701; 194-239*.
24. Ma CM, Rogers DWO, and Walters B (2001) DOSXYZnrc User's Manual. *NRC Report PIRS 509b (revF)*.
25. Patel NP, Shukla R, Balasubramanian N, Atri R, Dhull AK, Yadav HP, Kaushal V (2016) Radiation beam characterization and dosimetry of Theratron Equinox-80 telecobalt machine using BEAMnrc Monte Carlo simulation code. *International Journal of Medical Physics, Clinical Engineering and Radiation Oncology,* ***5(4)****: 298-316*.